Respiratory Research

RESEARCH

Open Access

Geranylgeranyl diphosphate synthase deficiency impairs efferocytosis and resolution of acute lung injury

Jiajia Jin[1,2†], Lihong Ma[1,3†], Lulu Li[2†], Xinyu Zhou[4], Suhua Zhu[2], Kaikai Shen[4], Qiuli Xu[5], Bei Jiang[6], Yanli Gu[7], Qianshan Ding[8], Hong Qian[9*], Tangfeng Lv[1,2,4*] and Yong Song[1,2,4*]

Abstract

Acute respiratory distress syndrome (ARDS) are major causes of mortality of critically ill patients. Impaired macrophage-mediated clearance of apoptotic cells (efferocytosis) in ARDS contributes to prolonged inflammation, yet the underlying mechanisms remain unclear. In this study, we investigated the role of geranylgeranyl diphosphate synthase (GGPPS) in efferocytosis during lung injury resolution. We identified dynamic changes in GGPPS expression in lung macrophages and circulating monocytes throughout the progression and resolution phases of acute lung injury (ALI). Myeloid-specific GGPPS knockout mice exhibited prolonged lung inflammation, increased accumulation of apoptotic neutrophils, a higher number of recruited macrophages, and a reduced number of resident macrophages. Notably, recruited macrophages play a dominant role in efferocytosis compared to resident macrophages. GGPPS deficiency suppressed efferocytosis in both macrophage subsets in vivo and in vitro. Mechanistically, GGPPS knockout disrupted AXL signaling in recruited macrophages. Importantly, administration of geranylgeraniol (GGOH) rescued the delayed resolution of lung injury, restored efferocytosis, and increased the suppressed AXL expression in CKO mice. Collectively, this study identifies GGPPS as a key regulator of AXL-mediated efferocytosis in recruited macrophages, highlighting its potential as a therapeutic target to accelerate ARDS resolution.

Keywords Acute respiratory distress syndrome, Resolution, Efferocytosis, Macrophage, Geranylgeranyl diphosphate synthase, AXL

† Jiajia Jin, Lihong Ma and Lulu Li jointly supervised the work.

*Correspondence:
Hong Qian
1016090565@qq.com
Tangfeng Lv
TangfengLv7210@nju.edu.cn
Yong Song
yong.song@nju.edu.cn
[1] Department of Respiratory and Critical Care Medicine, Jinling Hospital, Nanjing Medical University, #305, East Zhongshan Road, Nanjing 210002, China
[2] Department of Respiratory and Critical Care Medicine, Jinling Hospital, Nanjing 210002, China
[3] Department of Respiratory and Critical Care Medicine, Wuxi No. 2 People's Hospital, Wuxi 214086, China
[4] Department of Respiratory and Critical Care Medicine, Jinling Hospital, Nanjing University, Nanjing 210002, China
[5] Southeast University Medical College, Jinling Hospital, Nanjing 210000, China
[6] Department of Respiratory and Critical Care Medicine, Jinling Hospital, Nanjing University of Chinese Medicine, Nanjing 210000, China
[7] Department of Respiratory and Critical Care Medicine, The Affiliated Huaian No.1 People's Hospital, Nanjing Medical University, Huai'an 223000, China
[8] Nanjing First Hospital, affiliated with Nanjing Medical University, Nanjing 210006, China
[9] Department of Orthopaedic Surgery, Jinling Hospital, the First School of Clinical Medicine, Southern Medical University, Nanjing 210002, China

New & noteworthy

The mortality rate of ALI/ARDS is high, whereas the therapeutic choice is limited. Exploring the mechanism of lung injury resolution is key to identify therapeutic targets. Our findings showed a beneficial effect of GGPPS on the resolution of lung injury. AXL-mediated efferocytosis in recruited macrophages could be the key mechanism.

Introduction

Acute lung injury (ALI) and acute respiratory distress syndrome (ARDS) are major causes of acute respiratory failure with high mortality. Despite extensive investigation into the pathogenesis of ARDS, therapy remains mainly supportive [1]. In the resolution phase of ARDS, infiltrated neutrophils undergo apoptosis and are subsequently phagocytosed by macrophages through a process known as efferocytosis[2, 3]. Efferocytosis involves three main steps: the recruitment of macrophages, recognition and binding of apoptotic cells, and subsequent internalization and degradation of targets [4–6]. A well-coordinated efferocytosis process could prevent the release of noxious neutrophil substances and reprogram macrophages towards an anti-inflammatory phenotype [2, 7, 8]. In ARDS patients and ALI mouse model, efferocytosis was suppressed [9, 10]. Notably, inefficient efferocytosis has been implicated in increased lung damage and poorer outcomes of ALI/ARDS [10, 11], whereas enhanced efferocytosis could accelerate the repair of lung injury [12]. The precise mechanism by which efferocytosis was regulated remains elusive.

Geranylgeranyl diphosphate synthase (GGPPS) in mevalonate pathway is an important branch enzyme which converts farnesyl diphosphate (FPP) to geranylgeranyl diphosphate (GGPP) [13]. The two downstream nonsteroidal isoprene products, FPP and GGPP, involve in prenylated modification of different GTPases. The dysregulated expression of GGPPS is involved in the development of diverse diseases including fatty liver disease [14], infertility [15], and diabetes [16]. We previously identified a role of GGPPS in the acute phase of ALI mouse model [17]. However, the role of GGPPS in efferocytosis and resolution of lung injury remains unknown. Of note, it has been reported that in the mouse model of bisphosphonate-related osteonecrosis of the jaw, supplement with geranylgeraniol (GGOH), a substrate analog for GGPP, could rescue macrophage efferocytosis and improve the bone healing [18], indicating that GGPPS could play a role in efferocytosis. To test the hypothesis, the impact of GGPPS deficiency on macrophage efferocytosis and lung injury resolution was investigated. Two populations of macrophages, resident and recruited macrophages, co-exist in the inflamed lung with distinct transcriptional and functional programming [19]. Thus, the effects of GGPPS deficiency on the count and efferocytotic capacity of the two macrophage subsets were also examined. This study identified GGPPS as a key positive regulator of efferocytosis in recruited macrophages and the resolution of ARDS.

Methods

Mice

C57BL/6, WT (GGPPS$^{fl/fl}$), and CKO (GGPPS$^{fl/fl}$LysM-cre) mice were purchased from GemPharmatech Co., Ltd. All animal experiments were carried out according to the China Council on Animal Care and approved by the Institutional Animal Care and Use Committee of Nanjing University.

Mouse ALI model

To establish ALI mouse model, mice (8–12 weeks, male) were anesthetized with tribromoethanol (30 μl/g, Meilunbio, China) and intratracheally instilled with LPS (Sigma, O55:B5, 0.5 mg/kg). In separate groups of mice, GGOH (Sigma, 25 mg/kg) was intraperitoneally injected on day 3 and day 4 of ALI. Mice were sacrificed 0, 1, 3, 5, or 7 days after LPS instillation. The right lungs were lavage with saline. The bronchoalveolar lavage fluid (BALF) cells were enumerated on an automated cell counter (Bio-Rad) or subjected to flow cytometry analysis. Or the cytospin samples of BALF cells were stained with Wright's Giemsa and analyzed by light microscopy. The left lungs were harvested for histological analysis.

BALF analysis

The concentration of total protein was quantified using BCA Protein Assay (Beyotime, China). The levels of IL-6, TNF-α, IL-1β, and IL-10 in BALF were measured using the ELISA kits (Servicebio, China) according to the manufacturer's instructions.

Histology, immunostaining, and lung injury scoring

The left lungs were fixed in a 4% paraformaldehyde solution overnight followed by paraffin embedding and sectioning. Slices were then stained with hematoxylin and eosin (H&E) or subjected to immunofluorescence as described previously [20, 21]. All antibodies were listed in Supplementary Table S1. ALI was scored as previously described [22].

Isolation of peripheral blood monocytes

Mouse peripheral blood monocytes was isolated using Mouse Peripheral Blood Monocyte Isolation Kit (TBD2011M, Tianjin, China) according to manufacturer's

instruction. Cell pellets were then used for subsequent RNA extraction and qRT-PCR analysis.

Induction of apoptotic neutrophils

This study was approved by Ethics Review Committee at Jinling hospital. Peripheral blood (6 ml, anticoagulated with EDTA) was acquired from consenting healthy volunteers (18–60 years old). Neutrophils were isolated using Histopaque-1077 (Sigma) and Histopaque-1119 (Sigma) according to the manufacturer's protocols. Then, the isolated neutrophils were exposed to UV irradiation (254 nm, UVS-26, 6-W bulb, 0.02 J/s/cm2) at a concentration of $2.5\times10\text{^}6$ cells/ml for 15 min and incubated at 37℃ for 2 h. Approximately 70% of neutrophils were apoptotic (Annexin V^+7-AAD^- cells) (Supplementary Fig. 1).

TUNEL staining

Terminal deoxynucleotidyl transferase dUTP nick end labeling (TUNEL) staining of mouse lung tissue on day 5 of ALI was performed using Tunel Assay Kit (Servicebio, China) following the manufacturer's protocols. Images were captured using fluorescent microscopy and analyzed using Image J software (National Institutes of Health, USA).

Assay of efferocytosis in vivo

Efferocytotic capacity was also assessed as the percentage of $Ly6G^+$ cells within macrophages, as determined by flow cytometry analysis. Efferocytosis was also analyzed after intratracheal (i.t.) instillation with apoptotic neutrophils. Apoptotic neutrophils were labeled with CFSE (Invitrogen) and then i.t. instilled into WT or CKO mice ($1.0\times10\text{^}7$ in 100 µl per mouse). 3 h later, BALF cells were harvested and analyzed by flow cytometry. The efferocytotic capacity was presented as the percentage of $CFSE^+$ cells within $F4/80^+$ macrophages [23].

Efferocytosis assay in vitro

Bone marrow-derived macrophages (BMDMs) and alveolar macrophages (AMs) were generated as described previously [17]. BMDMs or AMs (5×10^4 cells per well) were overlaid with apoptotic neutrophils (macrophages: neutrophils = 1: 5–1: 10) labeled with CFSE (Invitrogen, 0.5 µM) for 2 h. Then, BMDMs or AMs engulfing apoptotic neutrophils were analyzed by flow cytometry (the percentages of $CFSE^+$ in $F4/80^+$ cells). The gating strategy was shown in Supplementary Fig. 2. Efferocytosis in vitro was also evaluated by immunofluorescence analysis. CMTPX (Invitrogen)-labeled BMDMs were co-cultured with CESE-labeled apoptotic neutrophils. 2 h later, efferocytosis was quantified as the percentage of $CMTPX^+CESE^+$ cells. For pretreatment with GGOH or AXL inhibitor, BMDMs were treated with GGOH (10 µM, Sigma) 24 h or with R428 (2.5 µM, Selleck) 1 h prior to coincubation, respectively.

Flow cytometry

Briefly, cells were blocked with FcR Blocking Reagent (Miltenyi, Germany) for 10 min, and then immunostained with primary antibodies. To analyze apoptotic neutrophil-derived epitopes within macrophages, BALF cells were blocked and stained with the viability dye (Thermofisher), F4/80, CD11b and CD11c, followed by fixation with BD Cytofix/Cytoper solution (BD Biosciences) and permeabilization using 1 × BD Perm/Wash buffer (BD Biosciences). Finally, cells were stained with Ly6G. The ratio of $Ly6G^+$ cells in macrophages was determined as the efferocytotic level [24, 25]. Data were acquired on flow cytometry (Moflox XDP, Beckman) and analyzed with Flow Jo software (Tree Star, USA). All antibodies were listed in Supplementary Table S1.

Western blot

Protein extraction and evaluation of protein concentration were performed as described previously [22]. Proteins was loaded onto SDS-PAGE gels, transferred to PVDF membranes (Millipore, USA), incubated with antibodies, and reacted with ECL substrate. Protein bands were detected using the Scannning System (Tanon 5200, China) and quantified using ImageJ Software (NIH). All antibodies were listed in Supplementary Table S1.

Quantitative real-time PCR

Total RNA was extracted from BMDMs using TRIzol Reagent (Vazyme, China) and reverse-transcribed to cDNA using HiScript III RT SuperMix for qPCR kit (Vazyme, China). qRT-PCR was carried out using Cham Q SYBR Green PCR Master Mix (Vazyme, China). Relative mRNA expression of the target genes is calculated according to the $2^{-\Delta\Delta CT}$ methods. The primer sequences are listed in Supplementary Table S2.

Detection of GTP-Bound Rac1

Rac1 activities were determined using the GLISA kit (Cytoskeleton) according to the manufacturer's protocols.

Statistics

Data are expressed as the mean ± standard deviation. Statistical significance of differences was determined by unpaired Student's t test, one-way ANOVA test with Tukey's multiple comparison test, or two-way ANOVA test using the SPSS software versions 23.0 (IBM). P values were indicated as $^*p<0.05$, and $^{**}p<0.01$.

Results

GGPPS expression is dynamically modulated in lung macrophages following LPS exposure

Intratracheal instillation of 0.5 mg/kg of LPS evoked neutrophil-mediated lung inflammation and injury that peaked on Day 3, significantly alleviated on Day 5, and returned to baseline on Day 7 (Fig. 1A, B). Consistently, total cell count (Fig. 1C) and neutrophil count (Fig. 1D) in BALF also peaked on Day 3 and dramatically decreased on Day 5. There is marked expansion of the macrophage pool in the BALF during ALI that started on Day 3 and peaked on Day 5 (Fig. 1E). Lymphocyte influx began on Day 3 concurrent with macrophage and reached its highest point on Day 5 (Fig. 1F). Total protein concentration also peaked on Day 3 and trended downward on Day 5 (Fig. 1G), indicating Day 3 and Day 5 as the key time points to investigate lung injury resolution.

We next evaluated GGPPS expression after ALI onset. In the immunofluorescence assay, GGPPS expression in lung macrophages were decreased on Day 3 compared to Day 0, and significantly recovered by Day 5 (Fig. 1H, I). The mRNA expression of GGPPS in circulating monocytes was also significantly decreased on Day 3 compared to Day 0, with a subsequent increase on Day 5 compared to Day 3 (Fig. 1J). These results suggest that GGPPS could play a role in the resolution of lung injury.

Myeloid-specific GGPPS knockout impeded the resolution of lung injury

We next investigated the role of GGPPS in lung injury resolution using myeloid-specific knockout mice. The knockout efficiency in BMDMs was evaluated previously [17]. GGPPS knockout efficiency in AMs was also determined (Supplementary Fig. 3). The BALF cells in WT and CKO mice under homeostasis were evaluated previously [17]. GGPPS knockout did not affect total cell count, the percentages of macrophage and neutrophils, or the morphology of the macrophages in BALF under homeostasis.

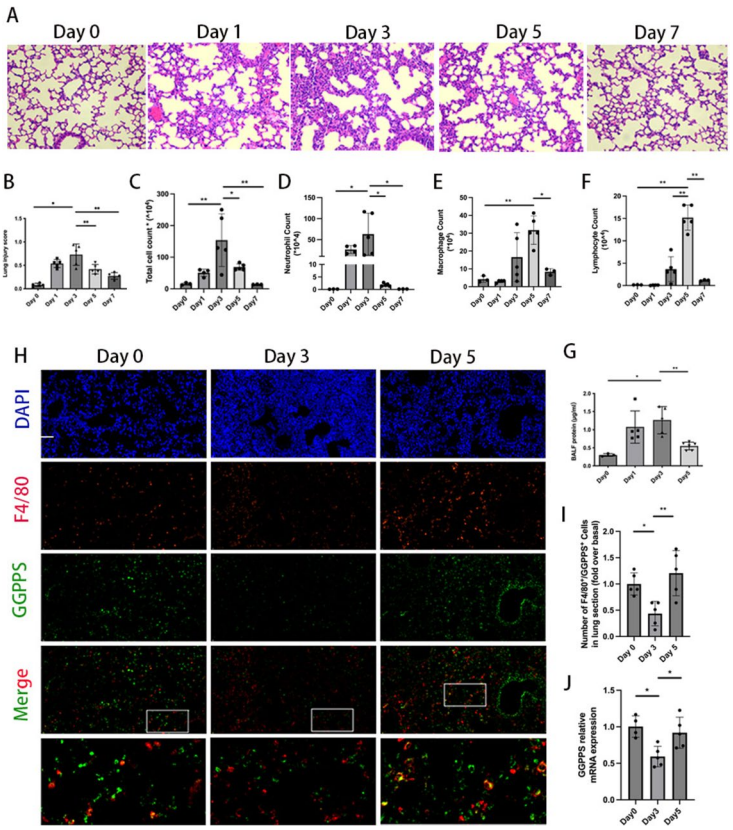

Fig. 1 GGPPS expression level in lung macrophages altered during the development and resolution of lung injury. Representative image (200×) of H&E staining of lung tissue (**A**), lung injury score (**B**), BALF total cell count (**C**), neutrophil count (**D**), macrophage count (**E**), lymphocyte count (**F**) and total protein level (**G**) of C57BL/6 mice after LPS instillation. Immunofluorescence staining for GGPPS (green) in macrophages (F4/80, red) was performed in lung sections on day 0, day 3, and day 5 following LPS instillation (**H**, **I**). Yellow spots indicate colocalization of GGPPS in lung macrophages. Representative images were shown. Scale bar = 100 μm. n = 3–6 mice for each group. The mRNA levels of GGPPS in circulating monocytes of mice on day 0, day 3, and day 5 after LPS instillation (**J**). For Fig J, each dot represents three mice to get enough RNA in monocytes. One-way ANOVA with the Turkey's multiple comparison test. *, $p < 0.05$, **, $p < 0.01$

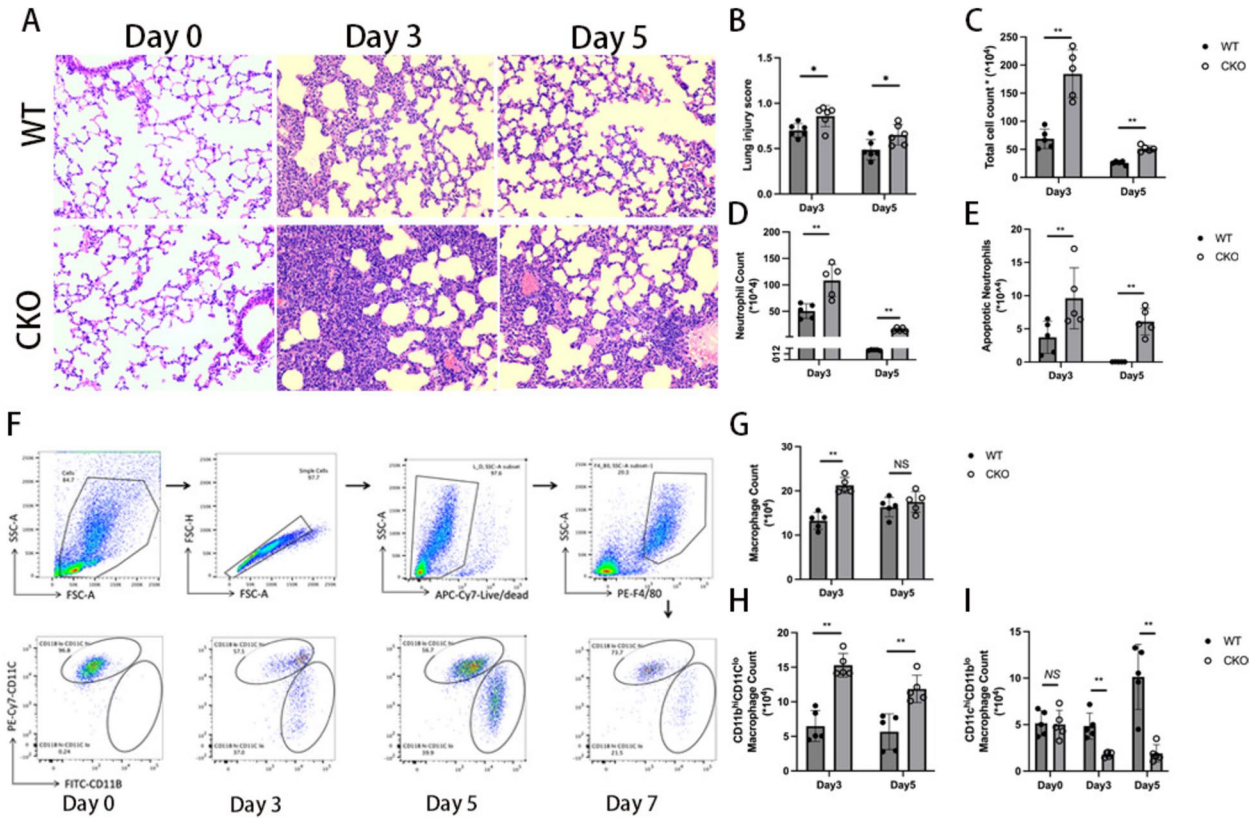

Fig. 2 GGPPS knockout impaired the resolution of lung injury. Representative image (200×) of H&E staining of lung tissue (**A**) and lung injury score (**B**) of WT and CKO mice 0d, 3d, and 5d after LPS instillation. Total cell count in BALF was enumerated on an automated cell counter (**C**). The count of neutrophils (**D**) and apoptotic neutrophils (**E**) in BALF of WT and CKO mice on Day 3 and 5. Gating strategy of BALF cells for macrophages ($F4/80^{+}$%, **F**), recruited macrophages ($CD11b^{hi}CD11c^{lo}$%, **F)**, and resident macrophages ($CD11c^{hi}CD11b^{lo}$%, **F**). The count of immune cells was calculated based on the total cell count and percentages (D, E, G, H, I). Student's t-test test, NS, not significant. *, $p < 0.05$, **, $p < 0.01$. $n = 3$–6 for each group

After LPS stimulation, CKO mice exhibited significantly higher ALI score compared to WT mice on Day 3 and 5 (Fig. 2A, B). The CKO group also displayed increased infiltration of total cells (Fig. 2C) and protein exudation (Supplementary Fig. 4A) in BALF on day 3 and Day 5. The levels of proinflammatory cytokines IL-6, TNF-α, and IL-1β were elevated in CKO group, whereas the level of pro-resolving cytokine IL-10 was significantly suppressed (Supplementary Fig. 4B, C). Furthermore, WT mice rapidly cleared apoptotic neutrophils. While the count of neutrophil (Fig. 2D, Supplementary Fig. 4D) and apoptotic neutrophils (Fig. 2E, Supplementary Fig. 4D) in CKO mice were significantly increased on Day 3 and 5. TUNEL staining also showed that obviously increased accumulation of $TUNEL^{+}$ cells in lung tissue in CKO mice compared to WT mice (Supplementary Fig. 4E, F).

Next, the impact of GGPPS deficiency on the macrophage pool in BALF was investigated. CKO group showed a significantly increased number of $F4/80^{+}$ macrophages compared to the WT group on Day 3. By Day 5, macrophage counts reached comparable levels in both groups (Fig 2F, G). The macrophage subsets, resident ($CD11c^{hi}CD11b^{lo}$) and recruited ($CD11b^{hi}CD11c^{lo}$) macrophages were further gated on $F4/80^{+}$ macrophages (Fig. 2F) as previously reported [19]. Consistently, macrophages were predominantly resident subset during homeostasis (referred to as Day 0). During acute and resolving inflammation, recruited macrophages exhibited robust accumulation on Day 3 and 5 followed by a progressive decline on Day 7. In comparison, resident macrophage levels remained constant during acute early inflammation and showed an increasing trend by Day 5 (Fig. 2F). Recruited macrophage counts was significantly increased in the CKO group on Day 3 and 5 compared to the WT group (Fig. 2H). In contrast, resident macrophages showed a notable reduction in CKO group (Fig. 2I). Taken together, these results indicated that GGPPS deficiency delays lung injury resolution, impairs the clearance of apoptotic neutrophils, and alters the distribution of macrophage subsets.

GGPPS knockout impaired efferocytosis in vivo

We next examined whether GGPPS deficiency affects efferocytosis in vivo. Intracellular Ly6G staining in macrophages was used to represent the level of efferocytosis [24, 25]. Interestingly, intracellular Ly6G staining in resident macrophages was poorer compared to recruited macrophages. Nonetheless, efferocytotic capacity of both macrophage subsets was significantly suppressed in CKO mice compared to WT mice (Fig. 3 A-C). Efferocytosis was also determined via i.t. instillation of apoptotic neutrophils (Fig. 3D). The percentage of $CFSE^+$ cells engulfed by CKO macrophages were significantly decreased compared to WT group (Fig. 3E, F). These results suggest that GGPPS promotes the resolution of lung injury by modulating macrophage efferocytosis.

GGOH rescued the impaired lung injury resolution of CKO mice

GGOH is a C20 isoprenoid that is found in fruits, vegetables, and grains, including rice [26, 27]. Besides, GGOH could be converted into GGPP in cells [20]. To further confirm the role of GGPPS in lung injury resolution, CKO mice with ALI was administered i.p. with GGOH on day 3 and day 4 (Fig. 4A). The impact of GGOH was validated through Western blot analysis to evaluate the

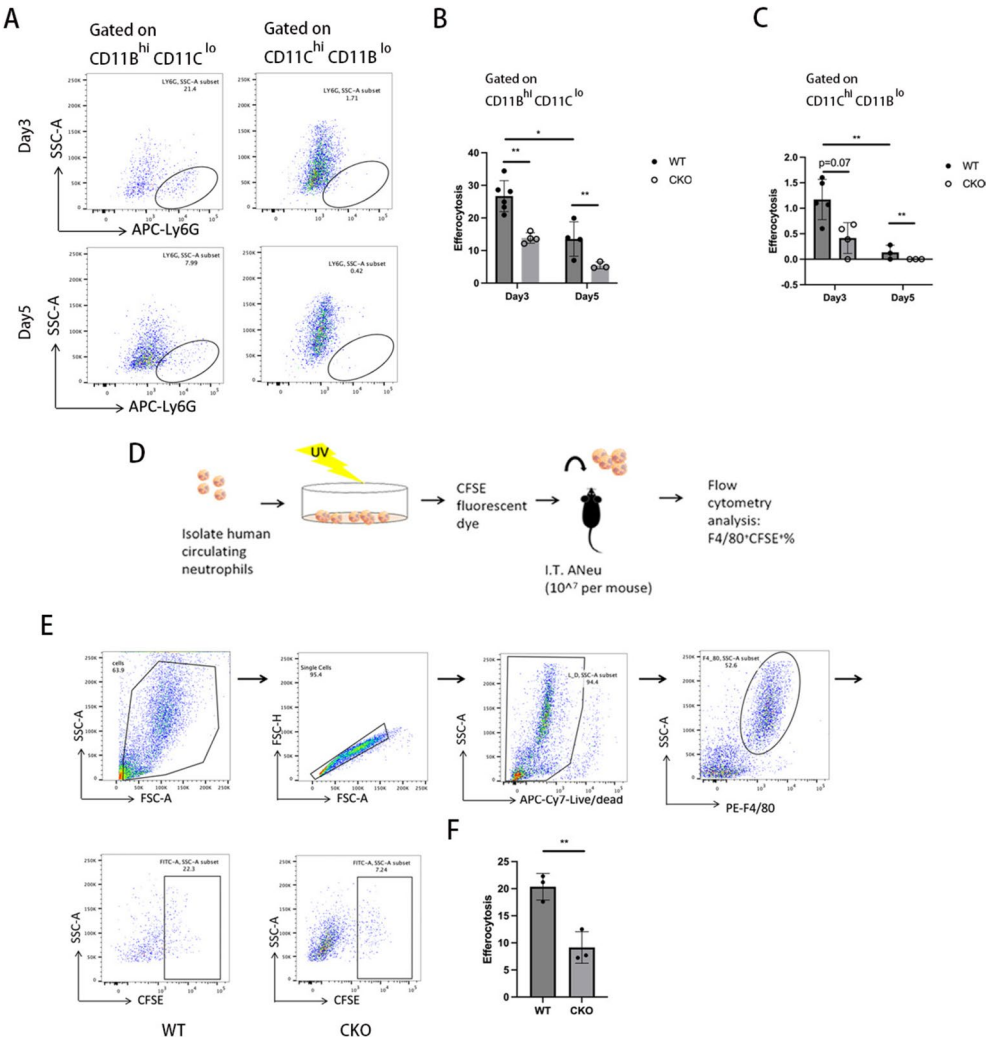

Fig. 3 GGPPS knockout impaired efferocytosis in vivo. Efferocytosis was evaluated by flow cytometry quantification of $Ly6G^+$ cells in $CD11b^{hi}CD11c^{lo}$ and $CD11c^{hi}CD11b^{lo}$ macrophages in BALF on Day 3 and 5 (**A**-**C**). $n = 3$–6 for each group. Student's t-test test, $^*p < 0.05$, $^{**}p < 0.01$. **D** Schematic diagrams showing the procedure of determining efferocytosis after i.t. instillation of apoptotic neutrophils. Efferocytosis was determined by flow cytometry quantification of uptake of CFSE-labeled apoptotic cells by macrophages (the percentage of $CFSE^+$ cells among $F4/80.^+$ cells) 3 h after i.t. instillation of apoptotic human neutrophils into WT or CKO mice (**E**, **F**). $n = 3$–6 for each group. Two-way anova analysis or Student's t-test test, *, $p < 0.05$, **, $p < 0.01$

expression of non-prenylated RAP1A in alveolar macrophages on Day 5. RAP1A was the representative geranylgeranylated protein and could be used to evaluate protein geranylgeranylation [28–30]. The protein level of unprenylated RAP1A was decreased after GGOH supplementation (Supplementary Fig. 5A, B), suggesting that GGOH was appropriately working. GGOH administration significantly decreased the lung injury score (Fig. 4B, C), total cell count (Fig. 4D), and neutrophil count (Fig. 4E) of CKO mice. The clearance of apoptotic neutrophils was also accelerated by GGOH treatment (Fig. 4F). Macrophage count was comparable between the two groups (Fig. 4G). Further analysis of macrophage subsets revealed that CKO + GGOH group exhibited significantly decreased number of $CD11b^{hi}CD11c^{lo}$ macrophage (Fig. 4H) and obvious increased $CD11c^{hi}CD11b^{lo}$ macrophage number (Fig. 4I). Importantly, the hampered efferocytotic capacity of recruited and resident macrophages in CKO mice were also rescued by GGOH (Fig. 4J-L). Thus, these results further suggested that GGPPS play an important pro-resolving role in ALI.

GGPPS deficiency impaired efferocytosis in vitro

We next investigated whether interfering GGPPS expression could affect efferocytosis in vitro (Fig. 5A). After co-incubation, $CFSE^{+}$% cells in CKO BMDMs were significantly decreased compared to WT BMDMs, which was rescued by GGOH pretreatment (Fig. 5B-C). The impact of GGOH on protein geranylgeranylation in BMDMs was also validated (Supplementary Fig. 5C, D). Efferocytosis was also evaluated in resident alveolar macrophages (AMs) in vitro, demonstrating that GGPPS knockout also suppressed clearance of apoptotic cells in AMs (Supplementary Fig. 6). Next, CMTPX-labeled BMDMs and CFSE-labeled apoptotic neutrophils were co-incubated for 2 h and IF assay also showed that the percentage of $CMTPX^{+}CFSE^{+}$ cells were significantly decreased in CKO BMDMs (Fig. 5D, E). These results further indicated that GGPPS is a positive regulator of efferocytosis.

Impaired efferocytosis resulted from GGPPS knockout was associated with disrupted AXL signaling

We next determined whether GGPPS knockout would affect the expression of efferocytosis-specific genes in BMDMs after 2 h of coincubation. Gene expression levels were determined for Cx3cr1, P2ry2, and S1pr1, which involve the recruitment of apoptotic cells; for Axl, Tyro3, Timp3, Pros1, Mertk, and Gas6, which mediate the recognition and binding of apoptotic cells by macrophages; and for Rac1, Elmo1, and Dock2, which contribute to apoptotic cell internalization. We found that several genes, including Cx3cr1, S1pr1, Axl, Timp3, Pros1, and Mertk, showed a downward trend in CKO BMDMs. Specifically, Axl was significantly downregulated in the knockout group (Fig. 6A). AXL is one of the best studied efferocytotic receptors and plays a key role in regulating efferocytosis in inflammatory diseases [21, 31]. Flow cytometry assay also showed that CKO group exhibited significantly reduced AXL expression, which was restored by GGOH treatment (Fig. 6B, C). The protein level of AXL in BMDMs via Western assay also showed similar downward trend in CKO group (Fig. 6D, E).

Our group previously found that GGPPS deficiency enhances Rac1 activity in macrophages in the acute phase of ALI [17]. Interestingly, Rac1 activation was reduced in the CKO group after co-incubation with apoptotic neutrophils, which contrasts with its response to LPS stimulation (Supplementary Fig. 7).

Next, AXL expression in macrophage subsets during lung injury was also determined. In WT mice, the percentage of AXL^{+} cells on $CD11b^{hi}CD11c^{lo}$ recruited macrophages was approximately 40% on Day 3, followed by a gradual increase on Day 5 and 7 (Supplementary Fig. 8). In contrast, AXL was constitutively expressed in the vast majority of resident macrophages. In CKO group, recruited and resident macrophages both exhibited decreased AXL expression compared to WT group (Fig. 6F, G). Besides, GGOH administration rescued the impaired AXL expression in both macrophage subsets (Supplementary Fig. 9). Finally, AXL inhibitor R428 was used. The impact of AXL inhibitor on the downstream signaling was determined through

(See figure on next page.)

Fig. 4 GGOH rescued the impaired lung injury resolution of CKO mice. **A** The schematic diagram showing the procedure of GGOH intervention after onset of ALI. Representative image (400×) of H&E staining of lung tissue (**B**) and lung injury score (**C**) of CKO mice with or without GGOH treatment. The total cells in BALF were enumerated on an automated cell counter (**D**). BALF neutrophils (**E**), apoptotic neutrophils (**F**), macrophages (**G**), $CD11b^{hi}CD11c^{lo}$ recruited macrophages (**H**), and $CD11c^{hi}CD11b^{lo}$ resident macrophages (**I**) of ALI mice in CKO and CKO + GGOH group. Gating strategy was shown in Fig. 2F. The count of immune cells was calculated based on the total cell count and percentages. The percentage of $CD11b^{hi}CD11c^{lo}$ recruited macrophages and $CD11c^{hi}CD11b^{lo}$ resident macrophages with intracellular $Ly6G^{+}$ staining in CKO and CKO + GGOH group (**J**-**L**). Student's t-test test, *, $p < 0.05$, **, $p < 0.01$

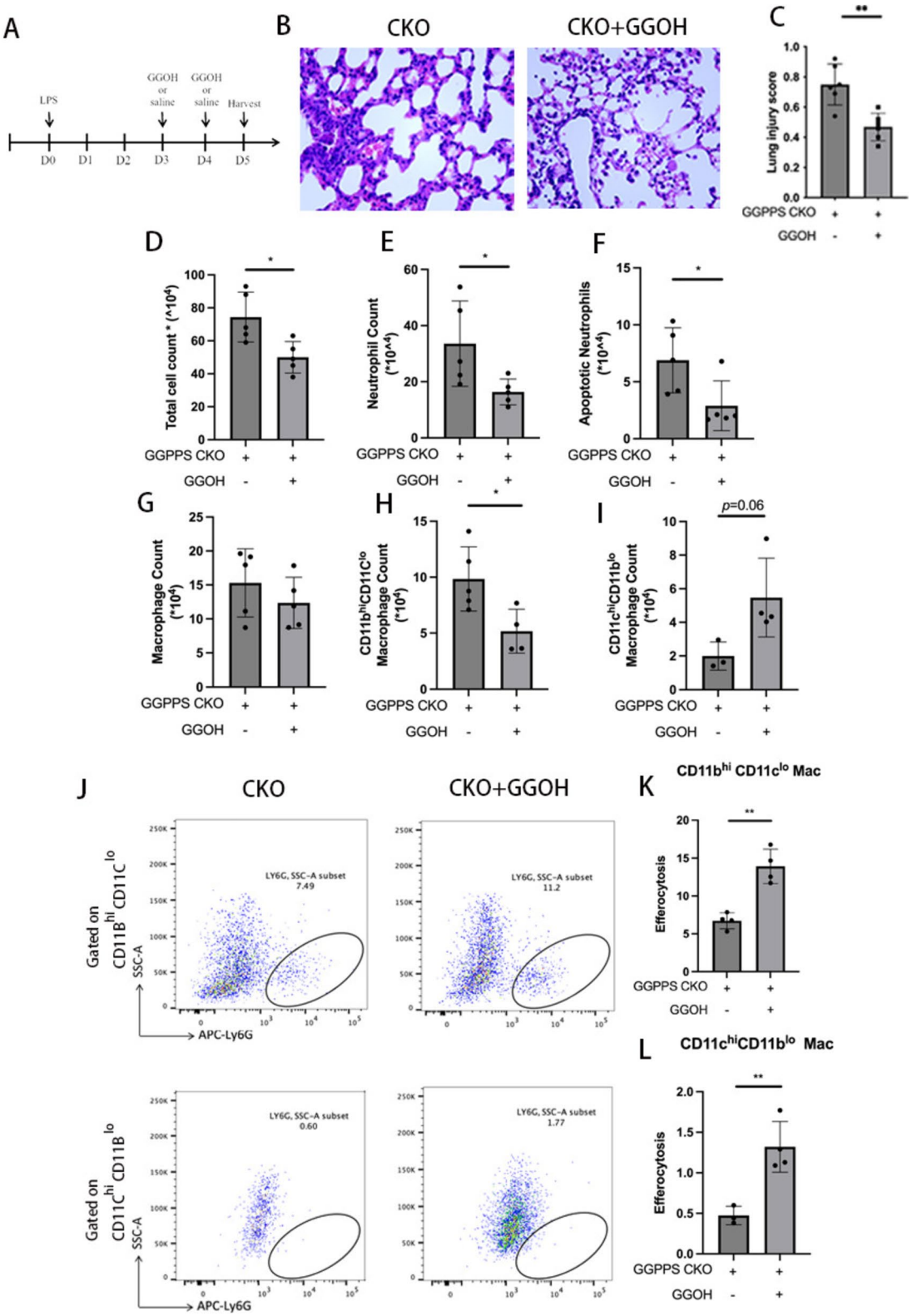

Fig. 4 (See legend on previous page.)

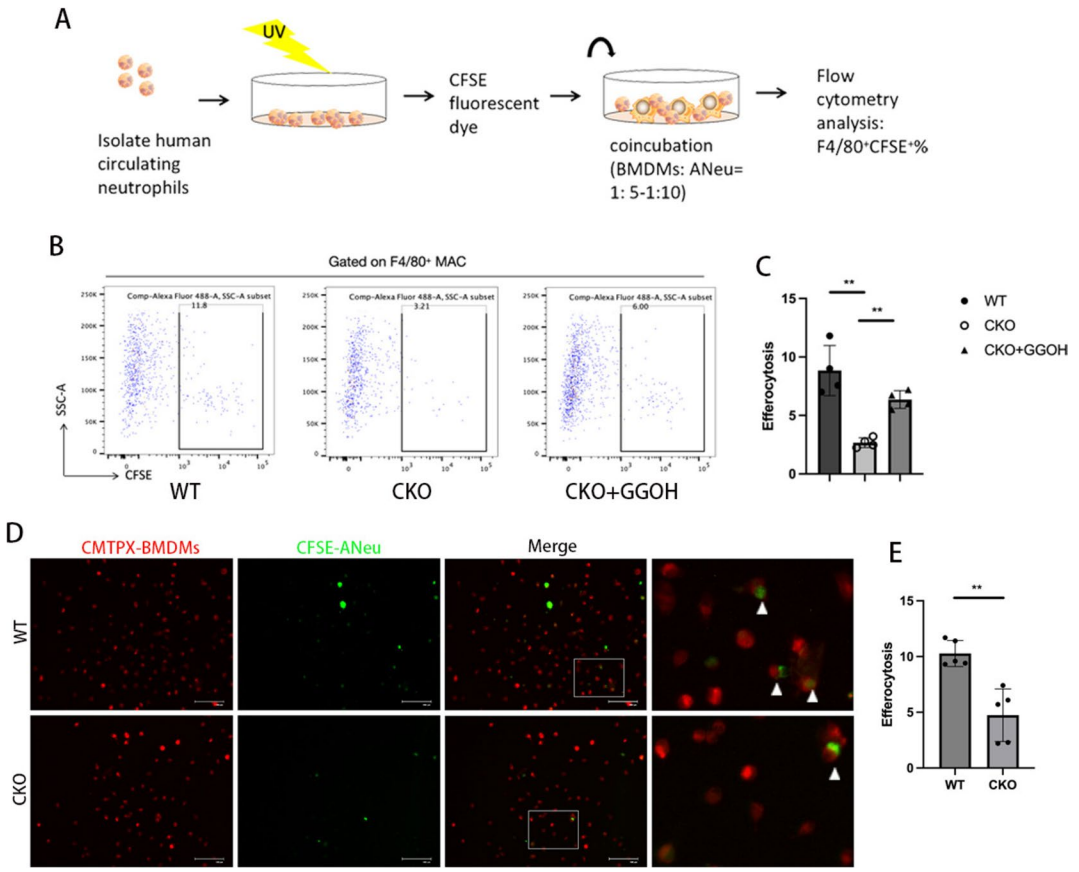

Fig. 5 GGPPS knockout impaired efferocytosis in vitro. Schematic diagrams showing the procedure of determining macrophage efferocytosis in vitro (**A**). Efferocytosis was determined by flow cytometry quantifying the percentage of $CFSE^+$ cells among $F4/80^+$ cells 2 h after co-incubation of apoptotic neutrophils and BMDMs (**B**). The percentage of $CFSE^+$ cells among $F4/80^+$ BMDMs after co-incubating WT, CKO and CKO + GGOH group (**C**). Microscopy images of CMTPX-labeled BMDMs and CFSE-labeled apoptotic neutrophils 2 h after co-incubation (**D**) and the quantification of efferocytotic macrophages ($CMTPX^+CFSE^+$% cells, **E**). Scale bar = 100 μm. n = 3–6 for each group. Student's t-test test, **, $p < 0.01$

determining Rac1 activity [32] (Supplementary Fig. 10). As expected, GGOH significantly increased the efferocytotic capacity of BMDMs, which could be reversed by AXL inhibitor (Fig. 6 H, I). In summary, these results suggest that GGPPS regulates efferocytosis via AXL signaling.

Discussion

This study demonstrates that myeloid-specific knockout of GGPPS in mice delays the resolution of lung injury. Recruited macrophages are the primary contributors to apoptotic cell clearance in acute lung injury. GGPPS deficiency impaired the phagocytosis of apoptotic neutrophils by recruited macrophages, both in vitro and in vivo. Importantly, reduced AXL activation may be a key mechanism underlying this inhibition. Therefore, this study identifies a novel role for GGPPS as a positive regulator of macrophage efferocytosis and the resolution of acute lung injury.

In this model, lung injury progressed and peaked on day 3, accompanied by reduced expression of GGPPS in lung macrophages and circulating monocytes, followed by the resolution of lung inflammation and a recovery of GGPPS expression. Although GGPPS is expressed in various lung cell types (Fig. 1H), our study specifically focuses on macrophage. Macrophages play a central role in tissue repair, including initiating phagocytosis of apoptotic neutrophils and releasing anti-inflammatory and pro-repair mediators [33]. In addition, the gradual recovery of GGPPS expression in macrophages suggests that GGPPS may play a significant role in initiating the resolution of lung injury. These findings support our rationale for targeting macrophages in the context of lung injury resolution. Notably, the decreased expression of GGPPS on Day 3 following LPS instillation may result from the infiltration of monocytes with lower GGPPS expression or from the downregulation of GGPPS in macrophages under inflammatory conditions. Future studies utilizing flow cytometry sorting assays will be necessary to

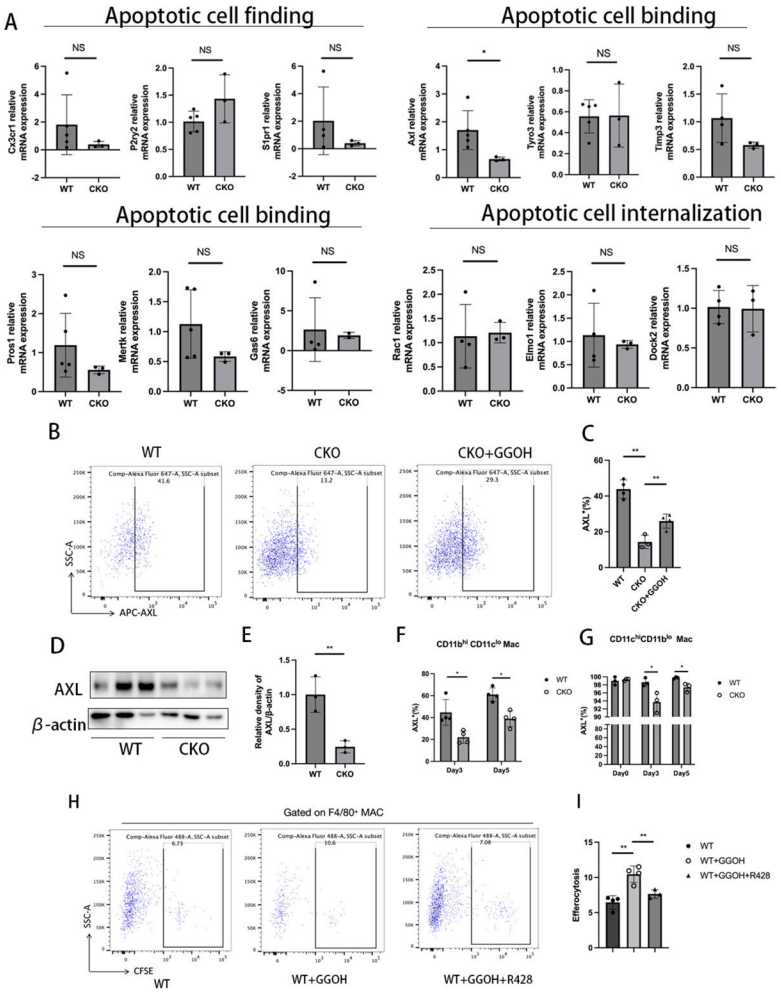

Fig. 6 Impaired efferocytosis resulted from GGPPS knockout was associated with disrupted AXL signaling. The mRNA levels of efferocytosis-associated genes in WT- or CKO-BMDMs were analyzed by qRT-PCR 2 h after co-incubation with apoptotic neutrophils (**A**). AXL expression in WT- or CKO- BMDMs were determined by flow cytometry (**B**-**C**) or by Western blot (**D**, **E**). The gating strategy was shown in Supplementary Fig. 2. AXL^+ cells in WT or CKO mice were analyzed by flow cytometry and quantified as the percentage AXL^+ cells in $CD11b^{hi}CD11c^{lo}$ recruited macrophages and $CD11c^{hi}CD11b^{lo}$ resident macrophages (**F**, **G**). Efferocytosis was determined by flow cytometry quantifying the uptake of CFSE-labeled apoptotic neutrophils by BMDMs in WT, WT + GGPP, and WT + GGPP + R428 group (**H**, **I**). $n = 3–5$ for each group. Student's t-test or one-way ANOVA analysis, *, $p < 0.05$, **, $p < 0.01$. NS, not significant

compare GGPPS expression levels among resident macrophages, recruited macrophages, and monocytes and to provide further insights into its regulation during inflammation.

Two macrophage subpopulations, resident AMs and recruited AMs, co-exist in the inflamed lung. The unique programming of resident and recruited alveolar macrophages during acute lung injury has been thoroughly examined [19, 32, 34, 35]. Resident AMs proliferate to replenish the AMs pool and maintain alveolar integrity. Recruited AMs amplify acute inflammation. They also contribute to resolving inflammation and restoring homeostasis. In our study, GGPPS knockout increased the number of recruited AMs while decreased the number of resident AMs. These results suggest the important and complex role of GGPPS in macrophage function, with the mechanisms regulating the function of different macrophage subsets warranting further investigation.

Impaired efferocytosis in patients with inflammatory lung injury is closely associated with increased morbidity and mortality [36]. Enhanced macrophage-mediated efferocytosis has been shown to accelerate the resolution of lung inflammation in an acute lung injury model induced by E. coli peritonitis [37]. In our study, the accumulation of apoptotic neutrophils in BALF and increased TUNEL staining in lung tissues of CKO mice prompted

us to investigate whether the delayed resolution observed in these mice was due to defective apoptotic cell clearance. We first performed intracellular staining of Ly6G in resident and recruited macrophages from WT and CKO mice. Notably, in alignment with previous studies [38–40], we observed that recruited macrophages in inflamed lungs were more efficient in apoptotic cell ingestion than resident macrophages. In vitro experiments also showed that BMDMs phagocytose apoptotic cells more efficiently than AMs. Janssen et al. [38] suggested that high levels of SP-A and SP-D surrounding resident macrophages might contribute to their poorer efferocytotic ability. However, the underlying mechanism requires further investigation.

This study demonstrated that GGPPS deficiency significantly impaired apoptotic cell clearance in both recruited and resident macrophages in vivo and in vitro. Considering efficient efferocytotic capacity of recruited macrophages, the recruited subpopulation could be the primary target of GGPPS. However, the correlation between GGPPS expression with the different efferocytotic capacity of the two macrophage subsets was unclear. Future study should include bone marrow transplantation experiments and create chimeras to clarify the role of GGPPS in efferocytosis of different macrophage subsets [38]. Additionally, we observed that resident macrophages displayed enhanced apoptotic cell uptake following intratracheal instillation of apoptotic cells, which could be attributed to differences in apoptotic cell burden. Specifically, as shown in Fig. 2E, the number of apoptotic neutrophils in BALF was approximately $10^{\wedge}5$, whereas the number of injected neutrophils reached $10^{\wedge}7$. Higher apoptotic cell burden promotes increased engulfment [41]. Taken together, given the dominant role of recruited macrophages in efferocytosis, further mechanistic experiments were performed primarily in BMDMs.

Efferocytosis is a tightly orchestrated process by which macrophages are recruited to sites of apoptotic activity, and then recognize, and finally engulf apoptotic cells [6]. Axl is one of the best studied recognition-related receptors [42]. Axl on macrophages binds to phosphatidylserine on the membrane of apoptotic cell via a bridging molecule, facilitating the tethering of these apoptotic cells [43]. This study demonstrated that GGPPS deficiency decreased the expression of AXL in BMDMs in vitro and recruited macrophages in vivo. The AXL inhibitor R428 suppressed the increased efferocytosis of BMDMs in WT + GGOH group. Consistently, Hu et al. [31] reported that AXL regulates efferocytosis function of microglia and alleviates early brain injury. In BMDMs, AXL-knockout mice also exhibited defective efferocytosis, enhanced M1 responses, and increased susceptibility to parasite infection [44]. These findings suggest that GGPPS deficiency diminished efferocytosis, at least in part, by intervening AXL signaling in recruited macrophages.

The temporal expression profile of AXL on resident and recruited macrophages during the ALI time course was also examined. AXL expression on recruited macrophages was around 40% on Day 3, followed by a gradual increase after the peak of inflammation. In contrast, AXL was constitutively expressed in the vast majority resident macrophages. GGPPS knockout also disrupted AXL expression on resident macrophages. Constitutive expression of AXL has been reported on resident macrophages in the mouse lung and AXL-deficient resident alveolar macrophages exhibited poorer efferocytosis in vitro [21]. The expression pattern of AXL on resident subset appears contradictory to its poor phagocytic ability, suggesting that surface expression of AXL is not the sole determinant of efferocytosis efficiency of resident macrophages during the resolution of lung injury. Post-translational modification, co-receptor interactions, or signaling inhibitors may limit its functional activity. Additionally, the excessive suppression of SP-A and SP-D on the efferocytosis of resident macrophages [38] may overshadow the pro-phagocytic function of AXL. This disparity deserves further investigation in future studies.

This study revealed that GGPPS deficiency suppressed the mRNA and protein expression of AXL. However, the potential pathways through which GGPPS modulates AXL mRNA expression remain unclear. Several transcription factors, including activator protein 1 (AP1) [45], Sp1/Sp3, and YAP [46], are known to act on the AXL promoter. Previous studies have shown that GGPPS knockout or statins, classic inhibitors of the mevalonate pathway, inhibit the transcriptional activity of AP1 [47], Sp1 [48], and YAP1 [49]. These findings suggest that GGPPS regulates AXL expression by targeting these transcription factors, warranting further studies to elucidate the underlying mechanisms.

The observed reduction in Rac1 activation (GTP-Rac1 levels) in CKO BMDMs following co-incubation with apoptotic cells appears contradictory to our previous findings demonstrating that GGPPS deficiency enhances Rac1 activation and promotes pro-inflammatory cytokine production in LPS-stimulated BMDMs [17]. This discrepancy suggests that protein prenylation may differentially regulate Rac1 activation in inflammatory versus efferocytosis pathways. As reported by Akula et al. [28], under inflammatory conditions, the guanine-nucleotide exchange factor (GEF) TIAM1 exhibits high affinity for non-prenylated Rac1, facilitating GTP loading and amplifying inflammatory responses in LPS-stimulated BMDMs. In contrast, efferocytosis employs a distinct Rac1 activation mechanism mediated by the

DOCK180/ELMO complex, another GEF subfamily that catalyzes GDP-to-GTP exchange on Rac1 [50–52]. Other Rac1 GEFs, including DbI [53] and Vav1 [54], were also identified to regulate Rac1 activity after engulfment of apoptotic cells. However, the precise role of Rac1 prenylation in efferocytosis remains poorly understood. Prenylated Rac1 is known to be crucial for endomembrane targeting and cytoskeletal reorganization during FcγR-mediated phagocytosis [55]. Besides, Rac1 activity could be restored by geranylgeraniol, thereby rescuing macrophage efferocytosis in bisphosphonate-related osteonecrosis of the mouse jaw [18]. Thus, we hypothesize that the DOCK180/ELMO complex, DbI, or Vav1, may preferentially recognize prenylated Rac1 during apoptotic cell clearance. Consequently, GGPPS deficiency could impair efferocytosis by disrupting the prenylation and activation of Rac1 in mouse ALI. This hypothesis warrants further studies systematically examining: 1) The role of Rac1 prenylation and activation in GGPPS-deficient macrophages in efferocytosis, using both in vitro and in vivo models; 2) Whether Rac1 inhibition abolishes the pro-efferocytotic effects of GGOH supplementation; 3) How Rac1 prenylation and activation vary across macrophage subsets and subcellular locations.

This study demonstrated that GGOH administration at the peak of inflammation restored AXL expression and the capacity of both recruited and resident macrophages to clear apoptotic neutrophils, and alleviated lung injury in GGPPS-CKO mice. These findings support the important role of GGPPS in resolution of ALI. GGOH, a natural C20 isoprenoid found in plants, has been shown to serve as a precursor for GGPP synthesis and protein isoprenylation in mammalian cells [20]. GGOH has demonstrated anti-inflammatory properties in human peripheral blood mononuclear cells [56] and in a mouse model of liver inflammation [57]. Additionally, GGOH enhanced macrophage efferocytosis and promoted the bone healing in the mouse model of bisphosphonate-related osteonecrosis [18]. However, GGOH administration did not exert therapeutic effects on WT mice with ALI (data not shown) in this study, though GGOH promoted efferocytosis of WT BMDMs in vitro. Notably, apoptotic neutrophils were efficiently cleared during Day 3 and 5 of acute lung injury in WT mice, enabling rapid resolution of lung injury. This may limit the potential for GGOH to exert its pro-resolving effects when administered on Days 3 and 4. Future studies should optimize the timing and dosage of administration to explore the protective role of GGOH.

Some limitations of our study should be addressed. First, clinical data were lacking. Evaluating GGPPS expression in alveolar macrophages from ARDS patients with successful versus failed resolution could provide valuable insights. This clinical investigation is currently ongoing. In addition, Lyz2-Cre driver system could also induce GGPPS deletion in neutrophils [58]. According to the Immunological Genome Consortium, GGPPS is expressed in neutrophils and to a similar degree as monocytes. Our data demonstrated that GGPPS deficiency increases neutrophil counts at both day 3 and 5 during ALI (Fig. 2D). The findings suggest that accumulated neutrophils could be due in part to defective efferocytosis, and it could also arise from increased recruitment or prolonged survival of neutrophils. Therefore, the potential role of GGPPS in regulating neutrophil survival and recruitment requires further investigation. Furthermore, though instillation methods and co-culture methods were traditional approaches for studying efferocytosis [23, 41, 59, 60], using human neutrophils to assess efferocytosis of mouse macrophage has certain limitations. Some key efferocytosis receptors and bridging molecules may have different affinities between species. However, the yield of thymocytes from mice or neutrophils from peripheral blood is relatively low, which increases the costs. To address these limitations, this study has incorporated in vivo experiments to validate the results.

Conclusions

In summary, GGPPS deficiency in macrophages delayed lung injury resolution. Reduced AXL expression and impaired efferocytosis in recruited macrophages could be the key mechanism. Thus, GGPPS-AXL signaling might provide promising therapeutic strategy for ARDS.

Supplementary Information

The online version contains supplementary material available at https://doi.org/10.1186/s12931-025-03241-6.

Additional file 1: Supplementary Figure 1. The percentage of apoptotic neutrophils was determined by flow cytometry (Annexin $V^+7\text{-}AAD^-$% cells). Supplementary Figure 2. Gating strategy to identify the percentage of $CFSE^+$ cells and AXL^+ cells in $F4/80^+$ BMDMs or AMs after co-incubation with apoptotic neutrophils. Supplementary Figure 3. The mRNA expression of GGPPS determined by qRT-PCR and the protein expression by Western blot in AMs of WT or CKO mice. Student's t-test, **, $p<0.01$. Supplementary Figure 4. The concentrations of total protein in BALF (A) determined by BCA assay and the concentration of cytokines (B, C) in BALF determined by ELISA in WT and CKO mice 3d and 5d after LPS instillation. Gating strategy of BALF cells for the neutrophils ($Ly6G^+$%, D), apoptotic neutrophils (Annexin$V^+7\text{-}AAD^-$%, D). Apoptotic cells were assessed by TUNEL staining of lung tissue of ALI mice on day 5 from the WT and CKO group (E). Scale bar=100 μm. The percentage of TUNEL+ cells was presented (F). Student's t-test, *, $p<0.05$, **, $p<0.01$. n=3-8 for each group. Supplementary Figure 5. The protein expression non-prenylated RAP1A in AMs from ALI mice with or without GGOH administration (A, B) and in BMDMs in WT, CKO and CKO+GGOH group (C, D). Student's t-test or one-way ANOVA analysis, *, $p<0.05$, **, $p<0.01$. Supplementary Figure 6. Efferocytosis was determined by flow cytometry quantifying the percentage of $CFSE^+$ cells among $F4/80^+$ cells 2 h after co-incubation of apoptotic neutrophils and AMs (A, B). Student's t-test, **, $p<0.01$. Supplementary Figure 7. Rac1 activity was determined in WT- or CKO-BMDMs after

co-incubation with apoptotic neutrophils using G-LISA kit. Student's t-test, *, $p<0.05$. Supplementary Figure 8. AXL^+ cells gated on $CD11b^{hi}CD11c^{lo}$ recruited macrophages and $CD11c^{hi}CD11b^{lo}$ resident macrophages in BALF (A). AXL expression in $CD11b^{hi}CD11c^{lo}$ recruited macrophages in BALF of mice with ALI on Day 3, 5, and 7 (B) and $CD11c^{hi}CD11b^{lo}$ resident macrophages on Day 0, 3, 5, and 7 (C). n=3-5 for each group. One-way ANOVA analysis, **, $p<0.01$. Supplementary Figure 9. AXL expression in $CD11b^{hi}CD11c^{lo}$ recruited macrophages (A) and $CD11c^{hi}CD11b^{lo}$ resident macrophages (B) in BALF of ALI mice in CKO and CKO+GGOH group. n=3-5 for each group. Student's t-test, *, $p<0.05$. Supplementary Figure 10. Rac1 activity in BMDMs in WT, WT+GGPP, and WT+GGPP+R428 group was determined using G-LISA assay. n=3-5 for each group. One-way ANOVA analysis, *, $p<0.05$, **, $p<0.01$.

Additional file 2.

Acknowledgements
We thank Dr. Li Zhou for technical support.

Authors' contributions
Yong Song, Tangfeng Lv, and Hong Qian conceived and designed the experiments. Jiajia Jin, Lihong Ma, Lulu Li, Bei Jiang, and Yanli Gu carried out the experiments. Lihong Ma, Lulu Li, and Xinyu Zhou analyzed the data. Suhua Zhu, Kaikai Shen, and Hong Qian prepared the figures. Qiuli Xu and Qianshan Ding contributed to mouse breeding. Jiajia Jin, Tangfeng Lv and Yong Song interpreted the results. Jiajia Jin, Hong Qian, and Suhua Zhu drafted the manuscript. Tangfeng Lv and Yong Song revised the manuscript. All authors approved the final version of the manuscript.

Funding
This work was supported by the National Natural Science Foundation of China (Grant No. 82100095) and Jiangsu Province's Key Discipline (Grant No. JSDW202208).

Data availability
Data will be made available upon reasonable request.

Declarations

Ethics approval and consent to participate
This study was approved by Ethics Review Committee of Jinling Hospital (Clinical trial number, 2022DZKY-044–01; Registration Date, April 28, 2022).

Consent for publication
Not applicable.

Competing interests
The authors declare no competing interests.

Received: 18 November 2024 Accepted: 16 April 2025
Published online: 17 May 2025

References

1. Gorman EA, O'Kane CM, McAuley DF. Acute respiratory distress syndrome in adults: diagnosis, outcomes, long-term sequelae, and management. Lancet. 2022;400:1157–70.
2. McCubbrey AL, Curtis JL. Efferocytosis and lung disease. Chest. 2013;143:1750–7.
3. Boada-Romero E, Martinez J, Heckmann BL, Green DR. The clearance of dead cells by efferocytosis. Nat Rev Mol Cell Biol. 2020;21:398–414.
4. Elliott MR, Ravichandran KS. The dynamics of apoptotic cell clearance. Dev Cell. 2016;38:147–60.
5. Arandjelovic S, Ravichandran KS. Phagocytosis of apoptotic cells in homeostasis. Nat Immunol. 2015;16:907–17.
6. Noone PM, Reddy SP. Recent advances in dead cell clearance during acute lung injury and repair. Fac Rev. 2021;10:33.
7. Elliott MR, Koster KM, Murphy PS. Efferocytosis signaling in the regulation of macrophage inflammatory responses. J Immunol. 2017;198:1387–94.
8. Sachet M, Liang YY, Oehler R. The immune response to secondary necrotic cells. Apoptosis. 2017;22:1189–204.
9. Mahida RY, Scott A, Parekh D, Lugg ST, Hardy RS, Lavery GG, Matthay MA, Naidu B, Perkins GD, Thickett DR. Acute respiratory distress syndrome is associated with impaired alveolar macrophage efferocytosis. Eur Respir J. 2021;58:2100829.
10. Grégoire M, Uhel F, Lesouhaitier M, Gacouin A, Guirriec M, Mourcin F, Dumontet E, Chalin A, Samson M, Berthelot LL, et al. Impaired efferocytosis and neutrophil extracellular trap clearance by macrophages in ARDS. Eur Respir J. 2018;52:1702590.
11. Su K, Bo L, Jiang C, Deng X, Zhao YY, Minshall RD, Hu G. TLR4 is required for macrophage efferocytosis during resolution of ventilator-induced lung injury. Am J Physiol Lung Cell Mol Physiol. 2021;321:L787-l801.
12. Kumaran Satyanarayanan S, El Kebir D, Soboh S, Butenko S, Sekheri M, Saadi J, Peled N, Assi S, Othman A, Schif-Zuck S, et al. IFN-β is a macrophage-derived effector cytokine facilitating the resolution of bacterial inflammation. Nat Commun. 2019;10:3471.
13. Muehlebach ME, Holstein SA. Geranylgeranyl diphosphate synthase: Role in human health, disease and potential therapeutic target. Clin Transl Med. 2023;13:e1167.
14. Liu J, Jiang S, Zhao Y, Sun Q, Zhang J, Shen D, Wu J, Shen N, Fu X, Sun X, et al. Geranylgeranyl diphosphate synthase (GGPPS) regulates non-alcoholic fatty liver disease (NAFLD)-fibrosis progression by determining hepatic glucose/fatty acid preference under high-fat diet conditions. J Pathol. 2018;246:277–88.
15. Zhu R, Wang J, Feng T, Hu X, Jiang C, Wang X, Li K, Sang Y, Hua Y, Sun H, et al. The alteration of RhoA geranylgeranylation and Ras farnesylation breaks the integrity of the blood-testis barrier and results in hypospermatogenesis. Cell Death Dis. 2019;10:450.
16. Jiang S, Shen D, Jia WJ, Han X, Shen N, Tao W, Gao X, Xue B, Li CJ. GGPPS-mediated Rab27A geranylgeranylation regulates β cell dysfunction during type 2 diabetes development by affecting insulin granule docked pool formation. J Pathol. 2016;238:109–19.
17. Jin J, Qian H, Wan B, Zhou L, Chen C, Lv Y, Chen M, Zhu S, Ye L, Wang X, et al. Geranylgeranyl diphosphate synthase deficiency hyperactivates macrophages and aggravates lipopolysaccharide-induced acute lung injury. Am J Physiol Lung Cell Mol Physiol. 2021;320:L1011–24.
18. Chen X, Zhu W, Xu R, Shen X, Fu Y, Cheng J, Liu L, Jiang H. Geranylgeraniol restores zoledronic acid-induced efferocytosis inhibition in bisphosphonate-related osteonecrosis of the jaw. Front Cell Dev Biol. 2021;9:770899.
19. Mould KJ, Barthel L, Mohning MP, Thomas SM, McCubbrey AL, Danhorn T, Leach SM, Fingerlin TE, O'Connor BP, Reisz JA, et al. Cell origin dictates programming of resident versus recruited macrophages during acute lung injury. Am J Respir Cell Mol Biol. 2017;57:294–306.
20. Crick DC, Andres DA, Waechter CJ. Farnesol is utilized for protein isoprenylation and the biosynthesis of cholesterol in mammalian cells. Biochem Biophys Res Commun. 1995;211:590–9.
21. Fujimori T, Grabiec AM, Kaur M, Bell TJ, Fujino N, Cook PC, Svedberg FR, MacDonald AS, Maciewicz RA, Singh D, Hussell T. The Axl receptor tyrosine kinase is a discriminator of macrophage function in the inflamed lung. Mucosal Immunol. 2015;8:1021–30.
22. Li L, Ma L, Qian H, Wang Z, Chen M, Wang C, Gu W, Lv T, Jin J: GGPPS Negatively Regulates the Formation of Neutrophil Extracellular Traps in Lipopolysaccharide-Induced Acute Lung Injury. Inflammation 2024.
23. Long ME, Eddy WE, Gong KQ, Lovelace-Macon LL, McMahan RS, Charron J, Liles WC, Manicone AM. MEK1/2 inhibition promotes macrophage reparative properties. J Immunol. 2017;198:862–72.
24. Liebold I, Al Jawazneh A, Casar C, Lanzloth C, Leyk S, Hamley M, Wong MN, Kylies D, Gräfe SK, Edenhofer I, et al. Apoptotic cell identity induces distinct functional responses to IL-4 in efferocytic macrophages. Science. 2024;384:eabo7027.
25. Wang Y, Zhang W, Xu Y, Wu D, Gao Z, Zhou J, Qian H, He B, Wang G. Extracellular HMGB1 impairs macrophage-mediated efferocytosis by suppressing the Rab43-controlled cell surface transport of CD91. Front Immunol. 2022;13:767630.
26. Muraguchi T, Okamoto K, Mitake M, Ogawa H, Shidoji Y. Polished rice as natural sources of cancer-preventing geranylgeranoic acid. J Clin Biochem Nutr. 2011;49:8–15.

27. Pan MH, Lai CS, Dushenkov S, Ho CT. Modulation of inflammatory genes by natural dietary bioactive compounds. J Agric Food Chem. 2009;57:4467–77.
28. Akula MK, Ibrahim MX, Ivarsson EG, Khan OM. Protein prenylation restrains innate immunity by inhibiting Rac1 effector interactions. Nat Commun. 2019;10:3975.
29. Chong D, Chen Z, Guan S, Zhang T, Xu N, Zhao Y, Li C. Geranylgeranyl pyrophosphate-mediated protein geranylgeranylation regulates endothelial cell proliferation and apoptosis during vasculogenesis in mouse embryo. J Genet Genomics. 2021;48:300–11.
30. Wang XX, Ying P, Diao F, Wang Q, Ye D, Jiang C, Shen N, Xu N, Chen WB, Lai SS, et al. Altered protein prenylation in Sertoli cells is associated with adult infertility resulting from childhood mumps infection. J Exp Med. 2013;210:1559–74.
31. Tang J, Jin Y, Jia F, Lv T, Manaenko A, Zhang LF, Zhang Z, Qi X, Xue Y, Zhao B, et al. Gas6 promotes microglia efferocytosis and suppresses inflammation through activating Axl/Rac1 signaling in subarachnoid hemorrhage mice. Transl Stroke Res. 2023;14:955–69.
32. Lemke G. Biology of the TAM receptors. Cold Spring Harb Perspect Biol. 2013;5:a009076.
33. Sheng YR, Hu WT, Chen S, Zhu XY. Efferocytosis by macrophages in physiological and pathological conditions: regulatory pathways and molecular mechanisms. Front Immunol. 2024;15:1275203.
34. Mould KJ, Jackson ND, Henson PM, Seibold M, Janssen WJ. Single cell RNA sequencing identifies unique inflammatory airspace macrophage subsets. JCI Insight. 2019;4:e126556.
35. Han W, Tanjore H, Liu Y, Hunt RP, Gutor SS, Serezani APM, Blackwell TS. Identification and characterization of alveolar and recruited lung macrophages during acute lung inflammation. J Immunol. 2023;210:1827–36.
36. Levy BD, Serhan CN. Resolution of acute inflammation in the lung. Annu Rev Physiol. 2014;76:467–92.
37. El Kebir D, Gjorstrup P, Filep JG. Resolvin E1 promotes phagocytosis-induced neutrophil apoptosis and accelerates resolution of pulmonary inflammation. Proc Natl Acad Sci U S A. 2012;109:14983–8.
38. Janssen WJ, McPhillips KA, Dickinson MG, Linderman DJ, Morimoto K, Xiao YQ, Oldham KM, Vandivier RW, Henson PM, Gardai SJ. Surfactant proteins A and D suppress alveolar macrophage phagocytosis via interaction with SIRP alpha. Am J Respir Crit Care Med. 2008;178:158–67.
39. Hu B, Sonstein J, Christensen PJ, Punturieri A, Curtis JL. Deficient in vitro and in vivo phagocytosis of apoptotic T cells by resident murine alveolar macrophages. J Immunol. 2000;165:2124–33.
40. Zuttion M, Parimon T, Yao C, Stripp BR, Wang Y, Soto CM, Ortega Z, Li X, Janssen WJ, Chen P. Interstitial macrophages mediate efferocytosis of alveolar epithelium during influenza infection. Am J Respir Cell Mol Biol. 2024;70:159–64.
41. Wu X, Wang Z, Shern T, Zhang H. Efferocytosis assay to quantify the engulfment and acidification of apoptotic cells by macrophages using flow cytometry. STAR Protoc. 2024;5:103215.
42. Doran AC, Yurdagul A Jr, Tabas I. Efferocytosis in health and disease. Nat Rev Immunol. 2020;20:254–67.
43. Meriwether D, Jones AE, Ashby JW, Solorzano-Vargas RS, Dorreh N, Noori S, Grijalva V, Ball AB, Semis M, Divakaruni AS, et al. Macrophage cox2 mediates efferocytosis, resolution reprogramming, and intestinal epithelial repair. Cell Mol Gastroenterol Hepatol. 2022;13:1095–120.
44. Rigoni TS, Vellozo NS, Guimarães-Pinto K, Cabral-Piccin M, Fabiano-Coelho L, Matos-Silva TC, Filardy AA, Takiya CM, Lopes MF. Axl receptor induces efferocytosis, dampens M1 macrophage responses and promotes heart pathology in Trypanosoma cruzi infection. Commun Biol. 2022;5:1421.
45. Mudduluru G, Leupold JH, Stroebel P, Allgayer H. PMA up-regulates the transcription of Axl by AP-1 transcription factor binding to TRE sequences via the MAPK cascade in leukaemia cells. Biol Cell. 2010;103:21–33.
46. Rankin EB, Fuh KC, Castellini L, Viswanathan K, Finger EC, Diep AN, LaGory EL, Kariolis MS, Chan A, Lindgren D, et al. Direct regulation of GAS6/AXL signaling by HIF promotes renal metastasis through SRC and MET. Proc Natl Acad Sci U S A. 2014;111:13373–8.
47. Wan B, Xu WJ, Chen MZ, Sun SS, Jin JJ, Lv YL, Zhan P, Zhu SH, Wang XX, Lv TF, Song Y. Geranylgeranyl diphosphate synthase 1 knockout ameliorates ventilator-induced lung injury via regulation of TLR2/4-AP-1 signaling. Free Radic Biol Med. 2020;147:159–66.
48. Louneva N, Huaman G, Fertala J, Jiménez SA. Inhibition of systemic sclerosis dermal fibroblast type I collagen production and gene expression by simvastatin. Arthritis Rheum. 2006;54:1298–308.
49. Benhammou JN, Qiao B, Ko A, Sinnett-Smith J, Pisegna JR, Rozengurt E. Lipophilic statins inhibit YAP coactivator transcriptional activity in HCC cells through Rho-mediated modulation of actin cytoskeleton. Am J Physiol Gastrointest Liver Physiol. 2023;325:G239–50.
50. Brugnera E, Haney L, Grimsley C, Lu M, Walk SF, Tosello-Trampont AC, Macara IG, Madhani H, Fink GR, Ravichandran KS. Unconventional Rac-GEF activity is mediated through the Dock180-ELMO complex. Nat Cell Biol. 2002;4:574–82.
51. Komander D, Patel M, Laurin M, Fradet N, Pelletier A, Barford D, Côté JF. An alpha-helical extension of the ELMO1 pleckstrin homology domain mediates direct interaction to DOCK180 and is critical in Rac signaling. Mol Biol Cell. 2008;19:4837–51.
52. Koubek EJ, Santy LC. Actin up: an overview of the rac GEF Dock1/Dock180 and its role in cytoskeleton rearrangement. Cells. 2022;11:3565.
53. Yurdagul A Jr, Subramanian M, Wang X, Crown SB, Ilkayeva OR, Darville L, Kolluru GK, Rymond CC, Gerlach BD, Zheng Z, et al. Macrophage metabolism of apoptotic cell-derived arginine promotes continual efferocytosis and resolution of injury. Cell Metab. 2020;31:518-33.e10.
54. Proto JD, Doran AC, Gusarova G, Yurdagul A Jr, Sozen E, Subramanian M, Islam MN, Rymond CC, Du J, Hook J, et al. Regulatory T cells promote macrophage efferocytosis during inflammation resolution. Immunity. 2018;49(666–77): e6.
55. Ueyama T, Eto M, Kami K, Tatsuno T, Kobayashi T, Shirai Y, Lennartz MR, Takeya R, Sumimoto H, Saito N. Isoform-specific membrane targeting mechanism of Rac during Fc gamma R-mediated phagocytosis: positive charge-dependent and independent targeting mechanism of Rac to the phagosome. J Immunol. 2005;175:2381–90.
56. Frenkel J, Rijkers GT, Mandey SH, Buurman SW, Houten SM, Wanders RJ, Waterham HR, Kuis W. Lack of isoprenoid products raises ex vivo interleukin-1beta secretion in hyperimmunoglobulinemia D and periodic fever syndrome. Arthritis Rheum. 2002;46:2794–803.
57. Giriwono PE, Shirakawa H, Ohsaki Y, Hata S, Kuriyama H, Sato S, Goto T, Komai M. Dietary supplementation with geranylgeraniol suppresses lipopolysaccharide-induced inflammation via inhibition of nuclear factor-κB activation in rats. Eur J Nutr. 2013;52:1191–9.
58. Clausen BE, Burkhardt C, Reith W, Renkawitz R, Förster I. Conditional gene targeting in macrophages and granulocytes using LysMcre mice. Transgenic Res. 1999;8:265–77.
59. Proto JD, Doran AC, Gusarova G, Yurdagul A Jr, Sozen E, Subramanian M, Islam MN, Rymond CC, Du J, Hook J, et al. Regulatory T Cells Promote Macrophage Efferocytosis during Inflammation Resolution. Immunity. 2018;49:666-77.e6.
60. Yoon YS, Kim SY, Kim MJ, Lim JH, Cho MS, Kang JL. PPARγ activation following apoptotic cell instillation promotes resolution of lung inflammation and fibrosis via regulation of efferocytosis and proresolving cytokines. Mucosal Immunol. 2015;8:1031–46.

Publisher's Note